On Domain Structure and Local Curvature in Lipid Bilayers and Biological Membranes

C. Gebhardt, H. Gruler, and E. Sackmann

Abteilung Experimentalphysik III, Universität Ulm

(Z. Naturforsch. **32 c**, 581–596 [1977]; received December 8, 1976)

Model Membrane, Liquid Crystal, Phase Separation, Curvature Elasticity, Defect Structure

The lateral lipid organization and the local surface curvature in small and giant bilayer vesicles of binary lipid mixtures were investigated. Mixtures of the following lipids are studied: Cholesterin, di-alcyl-lecithins, dioleyl-lecithin and di-alcyl-phosphatidic acid. The latter is considered as being representative of charged natural lipids (*e. g.* phosphatidyl serine or cardiolipin).

Three different experimental methods are compared: 1) The excimerfluorescence method, 2) the spin label technique and 3) the freeze fracture electron microscopy. The latter two methods yield information on the size of lipid precipitations. The surface curvature may be studied by electron microscopy. The essential experimental results are: (1) Mixtures of smectic phases of different symmetry undergo lateral phase separation. (2) The phase separation leads to a domain-like lateral lipid organization. (3) The domain structure is often accompanied by a variation in local curvature. (4) In membranes containing a charged lipid component, the domain structure may also be triggered by external charges (such as surface proteins). (5) two types of domains are observed: Circular domains (diameters of the order of several 100 Å) occur in mixtures of non-tilted fluid and rigid phases. Elongated domains (width $\sim$100 Å) are observed in mixtures of tilted and non-tilted phases. This domain pattern is characteristic for mixtures of lecithins and cholesterols.

The domain structure is explained by combining the theory of spinodal decomposition of alloys with the essential result of the orientational elastic model of membranes. The domain size calculated from this model agrees well with the experimental result. The periodic ripple structure observed between the pre- and the main transition is explained by generalizing the concept of spinodal decomposition to include the separation of phases which are only distinguishable (*e. g.* by the tilt angle). The width of the domains in equilibrium is explained in terms of the spontaneous curvature of the decoupled monolayer of a bilayer. Good agreement with the experimental result is obtained. The ripple phase is only a special case of the surface induced domain structures in ordinary liquid crystals. The defect structure of the ripple phase has been analysed in terms of its symmetry. A symmetry rule is established which leads to a model of lipid orientation.

Below the pretransition no periodic domain pattern is observed under normal conditions. But upon cooling a bilayer very rapidly a defect structure reminiscent of a screw dislocation is observed. This is expected for coupled biaxial monolayers.

I. Introductory Remark

The proper function of biological membranes is often dependent on a well defined lipid composition, both with respect to the structure of the polar head groups and of the apolar hydrocarbon chains. A prominent example is the membrane of the Red Blood Cell. The main phospholipid constituents of human erythrocytes are: sphingomyeline (26%), phosphatidylcholine (28%), phosphatidylethanolamine (27%) and phosphatidylserine (13%) (*cf* Fig. 1). According to van Deenen and de Gier [1] the first two types of lipids are mainly distributed in the outer monolayer, while the inner monolayer is composed primarily of the latter two components.

Requests for reprints should be sent to Prof. Dr. H. Gruler, Abteilung Experimentalphysik III der Universität Ulm, Oberer Eselsberg, *D-7900 Ulm*.

The fatty acid composition of these lipids is also rather universal [1]. A prominent explanation for this finding is that nature chooses a characteristic fatty acid composition in order to adjust the membrane fluidity to its function. In fact, the lateral mobility within the lipid moiety of biological membranes may differ over several orders of magnitude, *e. g.* from an average lateral mobility of 50 000 Å/sec in liver microsomes [2] to nearly complete immobilization in the outer monolayer of human erythrocytes [3].

It is more and more realized now that both the lipids and the proteins incorporated into the lipid bilayer of biological membranes exhibit a non-random distribution. Even in highly fluid membranes, enzymes may condense to form functional complexes (*e. g.* the cytochrome P 450/cytochrome P 450 reductase in liver microsomes [2]). Both experimental [2, 35] and theoretical [36] studies strongly

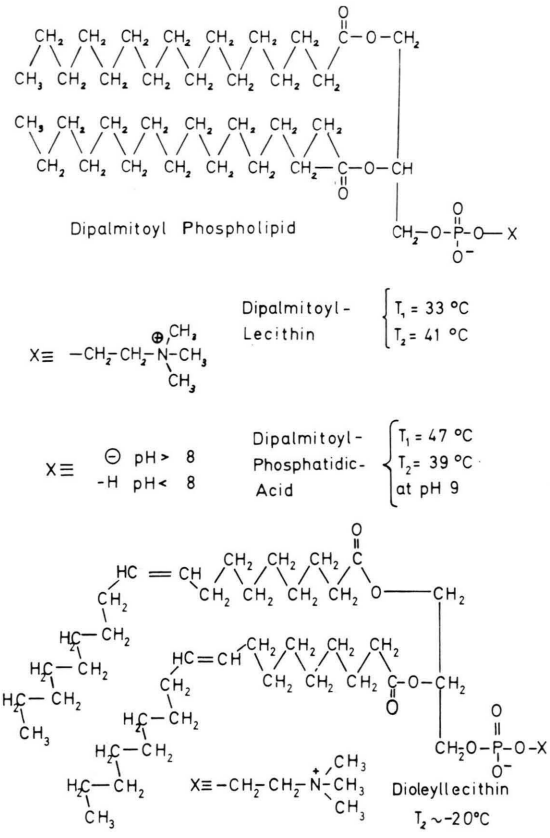

Fig. 1. Molecular structure of synthetic phospholipids representative of some important natural lipids. T_1, temperature of pre-transition, T_2, main transition temperature.

suggest that enzyme association may be effected by incorporation of the enzymes into rigid patches of lipid [2]. These lipid/protein entities may then swim as a whole in the fluid lipid matrix. A considerable membrane fluidity and a nonrandom distribution pattern of the membrane components seems to present a severe problem in membrane research. It has therefore been suggested that extrinsic membrane components, such as microfilaments and mitrotubuli, are mainly responsible for the protein distribution pattern in biological membranes [4, 5].

Now, the question arises whether the lipid moiety may play an active role in the lateral organization of membrane constituents. Stimulated by this question we studied the lateral lipid organization in simple model membranes of lipid alloys. In the present paper we report both experimental and theoretical evidence that phase separation in mixed lipid lamellae may lead to a domain-like lipid distribution. It is demonstrated that a high membrane fluidity and a non-random lipid distribution may be coexistent. The domain formation is a natural consequence of the differences in the symmetry of different polymorphical states of lipid lamellae.

II. Summary of Polymorphism of Lipid Bilayers

Membranes of the following three types of lipids or of mixtures of these lipids are primarily studied: dipalmitoyl lecithin (DPL), dimyristoyl lecithin (DML), dipalmitoyl phosphatidic acid (DPA) and dioleyl lecithin (DOL) (*cf* Fig. 1). Bilayer vesicles exhibit two first order thermotropic phase transitions [6, 7]: 1) the pretransition at a temperature T_1 and 2) the main transition at a higher temperature T_2. The monolayer vesicles seem to exhibit only the main transition in agreement with a recent theoretical model [8].

In close analogy to the situation found for thermotropic liquid crystals of the smectic class [9, 10], lipid bilayers may form structures of different symmetry which are separated by *first order* phase transitions. Several possible molecular structures of

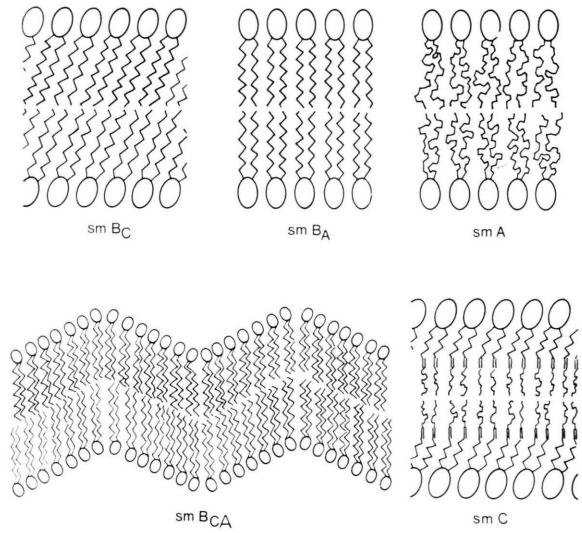

Fig. 2. Possible classes of two-dimensional smectic phases of lipid bilayers. The quasicrystalline smectic phases are given on the left side. They are characterized by the capital latter B (sm B). The lower suffixes, A, C and BA, denote the non-tilted, the tilted and the ondulated structure. The fluid phases are given on the right side. The capital letters A and C denote the non-tilted and the tilted structures. In the nomenclature of Tardieu *et al.* [12] the rigid phases sm B_C, sm B_A, sm B_{CA} are denoted as L_β, L_β', and P_β, respectively. The fluid phase sm A is called L_α.

the lipid bilayers are summarized in Fig. 2. In analogy to the nomenclature generally accepted for thermotropic liquid crystals, the different lipid structures are classified by the letters A, B and C: The smectic phases A and C are observed above the chain melting temperature and are often referred to as fluid (or liquid crystalline) phases [11]. The sm A phase is uniaxial, while the sm C phase is biaxial. The phases of type B are characteristic for paraffin-hydrocarbon chains in the *all-trans* configuration. The lipid molecules exhibit a long range order within the plane of the membrane [7, 12]. The hydrocarbon chains are supposed to form a triangular lattice [11]. The hydrocarbon chains may be either tilted (type B_C) or oriented perpendicularly (type B_A) with respect to the plane of the membrane. The tilted configuration may also exhibit an ondulated structure (called type B_{CA}) which is uniaxial on a macroscopic scale.

In the following the polymorphism of the lipids studied in this work is summarized.

Saturated lecithins: From the X-ray work [7, 12] it is now well known that at low temperatures (that is at $T < T_1$) DPL and DML are in the tilted rigid (smectic B_C) phase. This is also in agreement with a recent microscopic study of the ordered lamellar phase of DPL (at low water content) by Powers and Clark [13]. These authors demonstrated optical biaxiality of the multilamellar phase below the lower transition temperature. The observation of biaxiality on a macroscopic scale indicates that the lipid monolayers of the membranes must be strongly coupled in the low temperature phase. Above the lower transition the multilamellar system becomes uniaxial. The authors concluded from these findings that the uniaxial phase is of the smectic B_A type. However, it is clear that a bilayer of the smectic B_C type may appear nearly uniaxial if it assumes an ondulated (rippled) structure, the socalled B_{CA} phase in Fig. 2. Inspection of Fig. 1 of ref. 13 shows indeed that the uniaxial conoscopic interference pattern becomes rather grainy in the temperature region between the main- and the pretransition. This graininess may be caused by elastic distortions of the multilamellar system upon ondulation (*cf* ref. 16). The ondulated structure for multilamellar phases was postulated by Tardieu *et al.* [12] and by Janiak *et al.* [14].

Further insight in the nature of the smectic B phases may also be obtained from electron microscopy study using the freeze etching technique. So it was first shown by Verkleij *et al.* [15] that freezing a membrane from a temperature immediately below the main transition leads to the rippled structure. An electron micrograph of such a vesicle preparation is given in Fig. 3. It will be shown below that this texture may be explained in terms of the ondulated B_{CA} phase. If the vesicle is cooled from a temperature below T_1 the electron micrographs exhibit a smooth surface of the lipid layer (*cf* Fig. 8 a and ref. 14). DPL-bilayer vesicles thus exhibit the following polymorphism

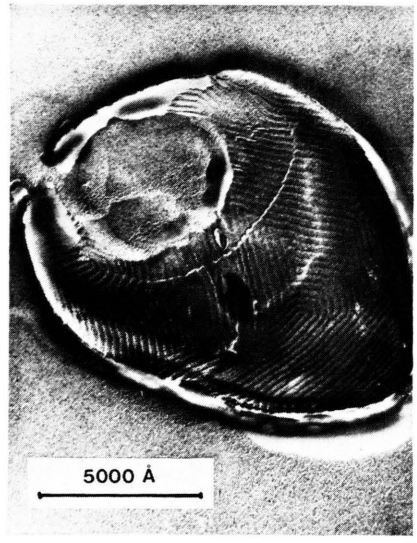

Fig. 3. Electron micrograph of a giant bilayer vesicle of dimyristoyl lecithin. Freeze etching technique was used by rapidly cooling from 20 °C. Magnification 125 000. The repeating distance of the ondulated structure is $\Lambda \approx 220$ Å. The defects of the wavelike pattern are discussed in Section IV E.

$$\text{sm } B_C \xrightarrow[T_1 = 33\,^\circ\text{C}]{} \text{sm } B_{CA} \xrightarrow[T_2 = 41\,^\circ\text{C}]{} \text{sm A}\,.$$

The corresponding transitions for DML are $T_1 = 15$ °C and $T_2 = 23$ °C.

Dipalmitoyl-phosphatidic acid: The bilayers show also two phase transitions. It is thus reasonable to conclude that the polymorphism of DPA at pH 9 is [17]

$$\text{sm } B_C \xrightarrow[T_1 = 39\,^\circ\text{C}]{} \text{sm } B_{CA} \xrightarrow[T_2 = 47\,^\circ\text{C}]{} \text{sm A}\,.$$

Charged lipids exhibit also lyotropic polymorphism. This is due to the strong dependence of the transition temperature on the charge of the polar head group [16]. At a given temperature the

DPA bilayers may be swept through the three different smectic phases by changing the pH. At $T = 55\ ^{\circ}C$ we found [19]

$$\text{sm } B_C \xrightarrow[pH = 4]{} \text{sm } B_{CA} \xrightarrow[pH = 7.8]{} \text{sm A}\,.$$

In the same way the DPA bilayers may undergo a transition from the smectic A to a rigid (probably smectic B) state by adsorption of external charges, such as positively charged polylysine or Ca^{2+} [17].

Dioleyllecithin: The structure of lipid lamellae of DOL is not well known yet. It is in a fluid state above $-20\ ^{\circ}C$. Since DOL is a bent molecule (*cf* Fig. 1 and Fig. 4 a) it is expected for topological reasons that it forms lipid bilayers of the smectic C type. This is consistent with the finding that the area per lipid molecule for DOL (80 Å^2 at 30 dyn and 40 °C) is only slightly larger than for DPL (70 Å^2 at 30 dyn and 40 °C).

III. Experimental Methods and Results

A) Preparation of vesicles

Large (giant) vesicles (1 μm diameter): The method of Reeves and Dowben [20] was applied: A 2 l Erlenmeyer flask was carefully cleaned with chromo-sulfuric acid. A solution of 3.5 mg lipid in 0.5 ml chloroform/methanol (1 : 2 volume ratio) was added. A very thin layer of lipid was deposited on the bottom of the flask by evaporation of the solvent under a stream of nitrogen. During evaporation the flask was rotated in a water bath kept at a temperature above the lipid phase transition. In order to obtain giant vesicles, the aqueous solution was slowly poured along the wall under slow rotation of the flask. The final concentration of lipid was 10^{-4} mol/l water. For illustration Fig. 3 shows a typical electron micrograph of such a giant vesicle prepared according to the freeze etching technique described below. The membrane broke along the interface separating the two monolayers of the bilayer vesicle. By cutting the vesicles into two halfs it could be verified that they were usually composed of bilayers. In some cases small vesicles were included in the large ones.

Small vesicles: Vesicles of diameter of about 400 Å were prepared in the usual way [11] by sonication of an aqueous lipid dispersion.

Monolayer vesicles: Vesicles enclosed by a lipid monolayer were prepared by sonication of an aqueous dispersion of the lipid and an organic phase as described earlier [11]. Sonication time was of the order of 10 minutes. Extended sonication leads to a loss of most of the organic phase. To adjust the density of the organic phase to a density $\varrho = 1.00$ a mixture of 63.6% *n*-hexane and 36.4% CCl_4 was used.

B) Spectroscopic evidence for domain structure

In previous work two spectroscopic methods were applied in an attempt to determine the microscopic lateral lipid distribution in binary mixed lipid bilayers and monolayers. In the following a brief summary of the essential results will be given.

1) The fluorescence method [17, 21] is based on the application of pyrene decanoic acid or pyrene as fluorescence probe. The basic physical process used is the formation of excited sandwich-like complexes (excimers) between a molecule in the ground state, P, and an excited probe molecule (P*) according to

$$P + P^* \overset{k_a c}{\rightleftarrows} (P\,P)^*\,.$$

The rate of complex formation is equal to the product of the 2nd order association constant k_a and the label concentration (per unit area). It is proportional to the ratio of the fluorescence intensities emitted by the monomer (I) and by the excimer (I'), respectively (*cf* ref. 21):

$$I'/I = K\,k_a \cdot c\,. \qquad (1)$$

For the application of excimer probes the following properties are essential:

α) In fluid lipid layers the complex formation is diffusion controlled. $k_a c$ is a direct measure for the rate of collisions, ν_c, of label molecules ($k_a c = \nu_c$). Measurements of I'/I as a function of c yields values of the mobility of the label in the plane of the membrane.

β) The solubility of pyrene decanoic acid in a lipid layer in the quasi-crystalline sm B_A or sm B_C states is extremely small. This property may be used to determine the critical temperatures an the widths of lipid phase transitions. In analogy to the application of TEMPO spin labels excimer probes are thus useful to observe conformational transitions involving phase separation in mixed membranes [17].

An example of such an application is given in Fig. 4. The intensity ratio I'/I (or the collision rate ν_c) is plotted as a function of temperature for pyrene decanoic acid in lipid bilayers a) of pure DPL, b) of pure DOL and c) of a 1 : 1 mixture of DOL and DPL. For DOL, the I'/I *versus* T plot

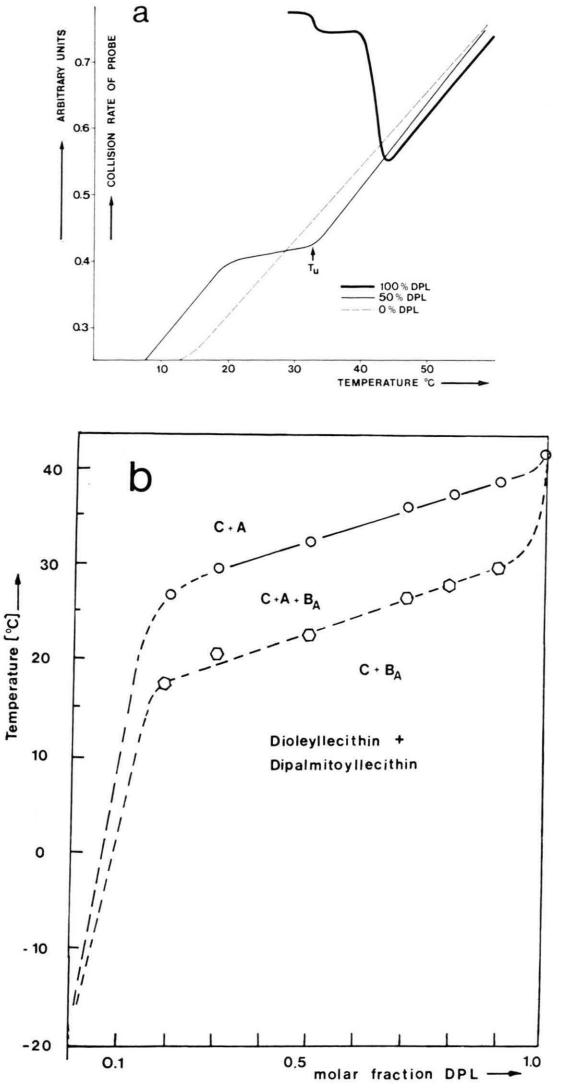

Fig. 4. Phase diagram of mixed membrane of dipalmitoyl lecithin (DPL) and dioleyl lecithin (DOL) as determined by the fluorescence label technique. (According to reference 26). a) Temperature dependence of rate of collision of pyrene decanoic acid probe (or excimer formation rate) in 1) a pure DPL-membrane (thick solid line), 2) a pure DOL-membrane (broken line) and 3) a 1 : 1 mixture of DOL and DPL (thin drawn line). The pure DPL-bilayers exhibit both the main transition at $T_2 = 41$ °C and the pretransition at $T_1 = 33$ °C. In the mixed system the deflection of the curve at the temperature T_u indicates the formation of regions of rigid smectic B_c phase of nearly pure DPL. b) Phase diagram of DOL/DPL system as obtained from plots of collision rate *versus* temperature for different compositions.

gives approximately a straight line between 18 °C and 50 °C * which is characteristic for a fluid lipid layer. The curve for DPL lamellae clearly indicates the main transition at 41 °C and the pretransition at 33 °C. The sharp increase in I'/I, observed at decreasing the temperature at T_2, is due to the very low solubility of the label in the smectic B state. This leads to the formation of clusters of label which have a very high excimer yield [21].

The mixed DOL/DPL membrane clearly exhibits a conformational change between 33 °C and 25 °C. The change in the slope of the I'/I *versus* T curve at decreasing temperature indicates the onset of phase separation at $T_u = 33$ °C. At this temperature regions of rigid lipid must be formed from which the label is squeezed out to a large extent. Therefore the label concentration in the fluid regions and therefore I'/I increases. The temperature of the onset of phase separation is only slightly decreased with respect to the DPL transition temperature ($T_2 \approx 41$ °C). Accordingly the rigid regions must contain a very high DPL concentration since the DOL chain melting transition occurs at -20 °C. It was pointed out by Tardieu *et al.* [12] that the smectic B phase of lipid mixtures tends to be non-tilted. We thus assume that the rigid regions are of the sm B_A type as indicated in the phase diagram in Fig. 4 b.

2) The spin label method was used several years ago to study the lipid organization [30] in phospholipid/steroid mixed membranes [11]. In this method one of the lipid components is labelled with a nitroxide free radical. The line shape of the Electron-Spin-Resonance spectra is then determined primarily by the spin exchange broadening. Computer simulation of the line shape yields values of the rate of spin exchange, the so called exchange frequency W_{ex}. W_{ex} is a direct measure for the degree of interaction of the labelled lipids. The exchange frequency is measured as a function of the composition of the mixture. Two limiting cases may be distinguished which are illustrated in Figs 5 a and 5 b.

α) The two lipid components (labelled and unlabelled) are randomized within the plane of the membrane. For fluid membranes, the ESR-spectra are slightly broadened at moderate concentration of labelled lipid. The broadening is directly related to the lipid lateral mobility. This situation is clearly characteristic for mixtures of labelled dipalmitoyl lecithin with unlabelled dipalmitoyl lecithin (DPL) or dimyristoyl-ethanolamine (DME) (*cf* Fig. 5). A

* The bent of the curve at 18 °C indicates a conformational change described already in ref. 23. The nature of this change is not understood yet.

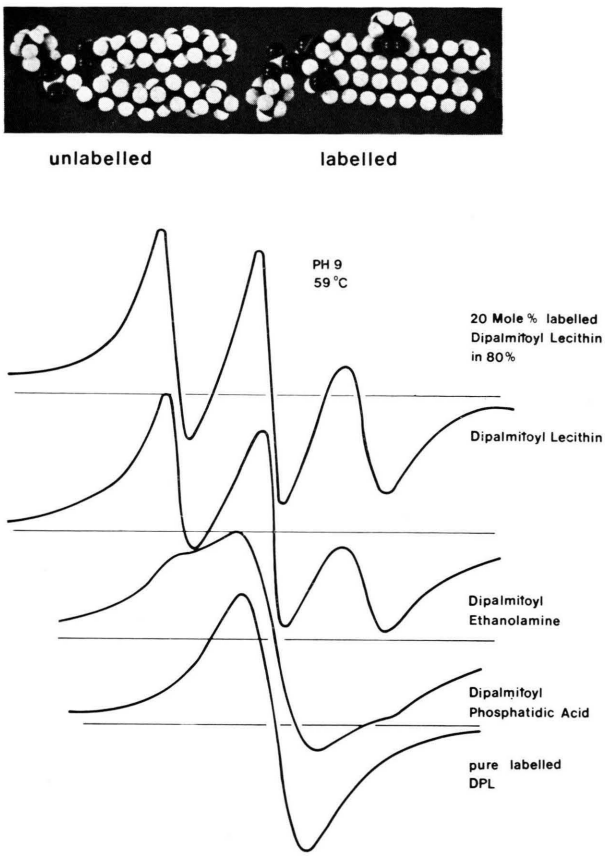

Fig. 5 a. Comparison of ESR-spectra obtained by mixing spinlabelled dipalmitoyl-lecithin with different lipids (upper three curves) with spectrum of pure labelled DPL (bottom spectrum). In all mixed systems the label concentration of 20 mol%.

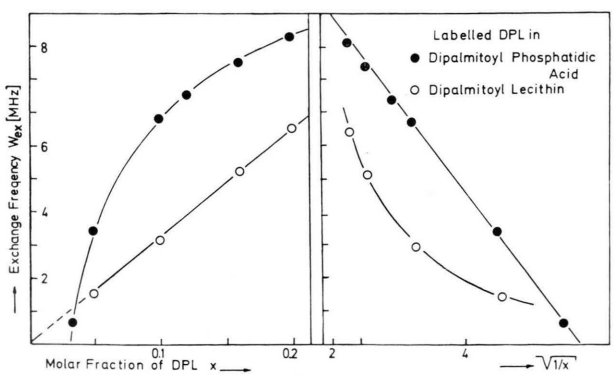

Fig. 5 b. Exchange frequency W_{ex} of mixture of labelled dipalmitoyl lecithin (DPL) with 1) DPL (circles ○) and 2) DPA (dots ●). The left side shows that for DPL W_{ex} is proportional to the molar fraction x_L of labelled DPL indicating a random mixture. According to the right side W_{ex} is proportional to $\sqrt{1/x_L}$ for DPA. This behavior is indicative of phase separation.

second characteristic feature of the fluid random mixture is the direct proportionality between $W_{ex} \propto x_L$ (*cf* Fig. 5 b for DPL).

β) Completely different behaviour is observed for a mixture of labelled DPL with DPA. Even at 20 mol% DPL-label, the three lines are nearly smeared out by exchange interaction. The spectrum closely resembles that obtained for a layer of pure labelled DPL. The exchange frequency ($W_{ex} \approx 6$ MHz) is by a factor of six larger than for a mixture of 20 mol% DPL-label in DPL (or DME). By using pyrene decanoic acid labels, we found that the lateral diffusion coefficient in DPA is only by about 30% higher than in DPL. This clearly demonstrates that DPL and DPA are only partially miscible at 59 °C. An identical result was obtained for monolayers of the 1 : 1 DPL/DPA mixture [17]. The latter experiments lead to the conclusion that the binary mixture of DPA and DPL exhibits a lateral phase separation at 59 °C(and pH 9). This is a most remarkable result since both DPL and DPA are in the fluid sm A state under these conditions. The inhomogeneity in the lateral lipid distribution is most clearly seen by plotting W_{ex} as a function of the molar fraction, x_L, of labelled lipid (*cf* Fig. 5 b). In the case of a nonrandom lipid distribution, W_{ex} is proportional to $\sqrt{1/x_L}$ as shown in reference [11]. Such a behavior is clearly shown by the DPL/DPA mixture above the chain melting transition of DPA.

The size of circular domains enriched in the labelled lipid component may be estimated from the slope of the straight lines [11, 24]. Some characteristic values for the DPL/DPA system are given in Table I for circular clusters. An essential result of such an interpretation is the finding, that the number of domains does not depend appreciably on the composition.

C) Chemically induced domain formation [17, 18, 24]

It may be considered a disadvantage of the spin label method that one chain of one of the lipid

Table I. Radius ϱ of circular clusters of labelled DPL in DPA for different molar fractions, x_L, of DPL. The concentration of DPL within the clusters is $x_L^c \approx 0.4$. N is the number of molecules per cluster.

x_L	0.10	0.20	0.30
ϱ	50	70	100
N	130	250	500

components is modified by the nitroxide group. The method is, however, most useful in demonstrating a striking property of mixed membranes containing one charged lipid component, such as DPA, phosphatidyl serine or cardiolipin: A lateral lipid segregation may be induced *isothermically* by external charges in the aqueous phase. An example is given in Fig. 6. It is clearly demonstrated that addition of positively charged poly-lysine or divalent ions (such as Ca^{2+}) leads to a dramatic increase in the spin exchange frequency. The same result is obtained for monolayer vesicles of the same mixture. Addition of Ca^{2+} to a membrane alloy containing

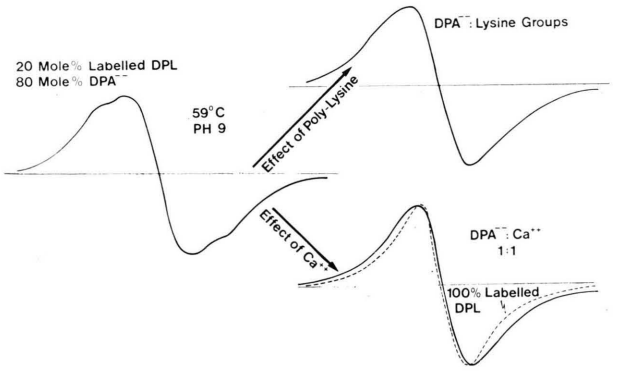

Fig. 6. Effect of external charges on ESR line shape of a 20 mol% mixture of labelled DPL in DPA. A strong increase in the mutual interaction of the labelled component is observed upon addition of both Ca^{2+} or positively charged poly lysine. This demonstrates that addition of the external charges enhances the separation of the two components DPL and DPA.

80% DPA^{2-} and 20% DPL leads to a complete lateral separation of the two lipid components [17] at an equimolar ratio of DPA^{2-} and Ca^{2+}. The observed ESR-spectrum closely resembles that of a bilayer of pure DPL-label (*cf* Fig. 6). From a plot of W_{ex} *versus* $1/x_L$ it follows that domains of pure DPL are formed [24]. For mixtures of DPA and *unlabelled* DPL this result has been confirmed by the fluorescence technique [17]. The complete separation of DPA and DPL is caused by a large shift in the transition temperature of DPA to higher temperatures upon the binding of Ca^{2+} to DPA^{2-} (at pH 9) [16, 18]. At 60 °C the DPA is transformed to the rigid (probably smectic B_A state). The sm A phase of DPL and the sm B phase od DPA^{2-} are completely immiscible.

The same effect is caused by poly lysine. As shown previously [24] binding of poly lysine to DPA^{2-} shifts the transition temperature to $T = 62$ °C at pH 9. At 59 °C, the membrane then consists of fluid domains of DPL and of rigid domains of DPA^{2-} bound by the charged polypeptide.

D) Electron microscopic evidence for domain structure

A more direct approach to the problem of domain structure in lamellae of lipid mixtures is the freeze etching technique first applied by Kleemann and McConnel to this problem [25]. The following preparation procedure was applied: First giant vesicles were prepared as described above. A small drop (10^{-1} cm diameter) of the vesicle preparation was put on a small round gold plate (~ 0.3 cm diameter). The plate was rapidly cooled (cooling rate about 10^2 °C/sec) by dipping it into liquified Freon 22 which was kept 40 °C above liquid nitrogen temperature. The frozen preparation was cut with a microtome in a Balzers freeze etching device. Etching was performed for about 100 sec at 5×10^{-6} mbar. Platinum/Carbon shadowing was performed under an oblique angle of 45° to a layer thickness of 30 Å. Subsequently a carbon layer of about 200 Å was deposited. The replica were observed with a Zeiss EM 10 Electron Microscope. In the following some results are summarized:

Fig. 7 a shows the electron micrographs of a large vesicle of dimyristoyl lecithin rapidly cooled a) from a temperature above the main transition ($T > T_2 \approx 23$ °C), b) from a temperature between the pretransition ($T_1 \sim 15$ °C) and the main transition and c) from a temperature below T_1. In the first and in the latter case a completely smooth membrane surface is obtained. Cooling from an intermediate temperature leads to the rippled surface already shown in Fig. 3. Obviously the phase, stable between T_1 and T_2, corresponds to the ondulated structure, the smectic B_{CA} state, mentioned above. The distance between the ripples is about 200 Å. The lines exhibit a characteristic defect structure explained below. Cooling from a temperature $T < T_1$ where a smectic B_C phase is expected leads to a smooth membrane surface. It is shown however, in the appendix A, that a defect structure may be observed, if the cooling process is much faster 10^{+6} °C/sec and is performed under higher mechanical strain.

The finding that the ondulated structure is clearly visible suggests that electron microscopy is a most sensitive technique to detect variations in the local

curvature of membranes. This technique should thus also allow to detect the lipid domain structure caused by phase separation in membrane alloys. In the following some results of such a study are summarized: Fig. 7 b shows the electron micrographs for giant bilayer vesicles of a 72 : 28 molar mixture of DML and cholesterol. The samples were also cooled from a temperature 1) below T_1, 2) between T_1 and T_2 and 3) above T_2 of DML. In the first two cases clearly visibly elongated domains are formed. The local curvature may have a triangular shaped cross section. This would correspond to the domain type of Fig. 10 b. This suggests that the domains are composed of DML in the tilted smectic B_C state. The width of the domains is of the order of 200 Å. The above conclusion is in ac-

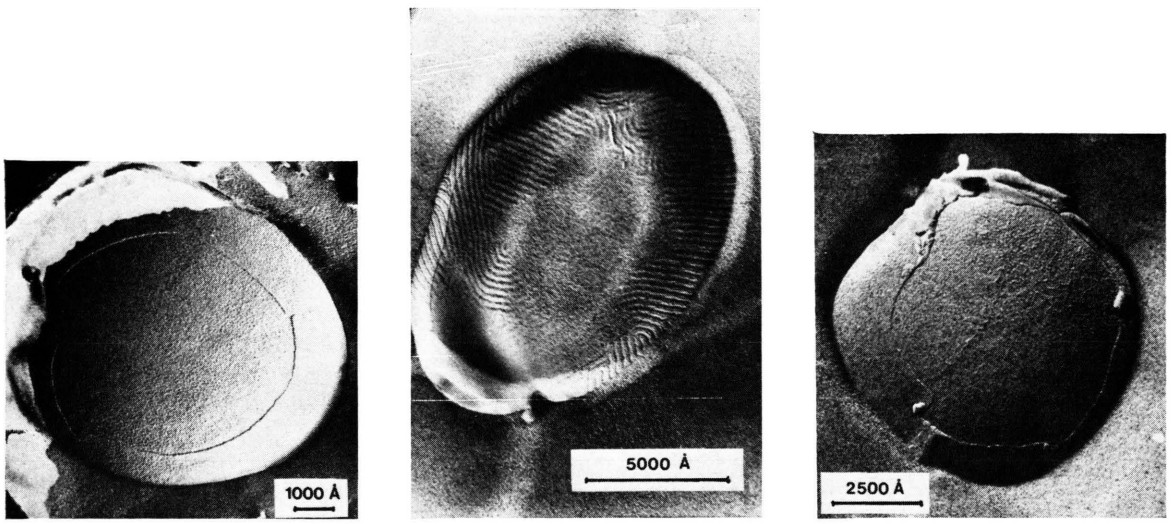

Fig. 7 a. Electron micrograph of large dimyristolyllecithin bilayer vesicles obtained by cooling from a temperature below the pretransition ($T<T_1$, left), between the transitions ($T_1<T<T_2$, centre) and above the main transition ($T>T_2$, right), respectively. A rippled structure is only obtained in the second case.

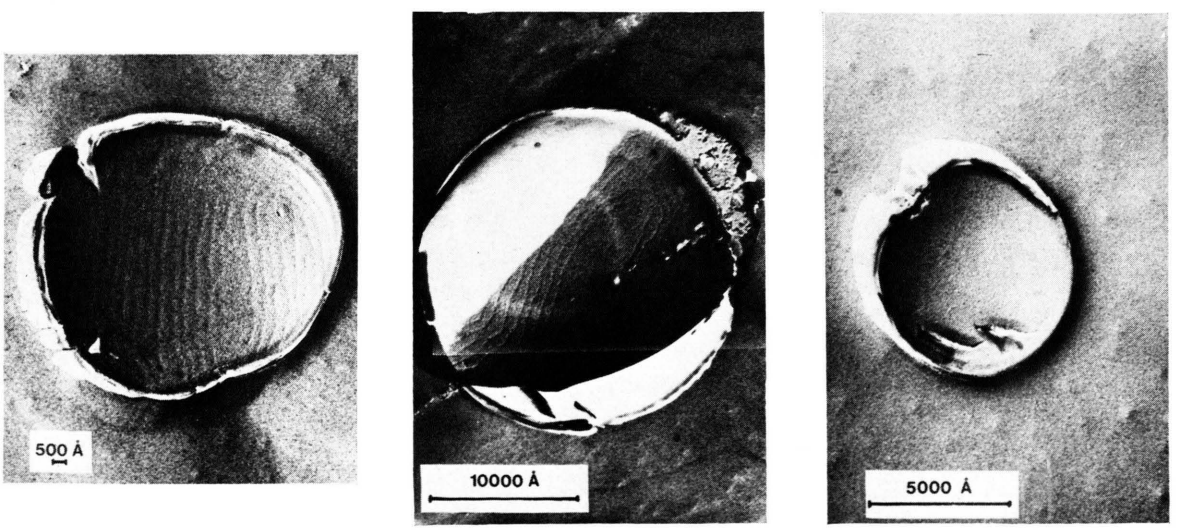

Fig. 7 b. Electron micrograph of bilayer vesicle containing 28 mol% cholesterol and 72 mol% DML. Mixture cooled from a temperature $T<T_1$ (left), $T_1<T<T_2$ (centre) and $T>T_2$ (right), respectively. The distances between the elongated domains are 350–450 Å for $T<T_1$ and 600 Å for $T_1<T<T_2$. Their width is about 100 Å in both cases. According to Fig. 10 b they are supposed to have a nearly triangular cross section. This suggests that the domains are formed from DML in the tilted smectic B_C state.

cordance with recent results of a monolayer study of two-dimensional lecithin/cholesterol mixtures [26]. In this work strong evidence was provided that at cholesterol concentrations below about 40% a lateral two-phase system is obtained. The lipid lamellae consist of regions composed of pure DML and of a 60 : 40 DML/cholesterol mixture, respectively. A domain structure was observed recently in a cholesterol/DPL mixture in an electron microscopy study of wet membranes by Hui and Parsons [39].

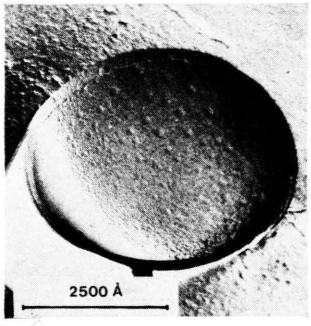

Fig. 8. Electron micrograph of a large bilayer vesicle (diameter about 1 μm) of a mixture of 65% dioleyl phosphatidic acid, 15% dioleyl lecithin and 20% cholesterol. Upon freeze etching the lipid bilayer was broken along the plane separating the two monolayers. The hydrophobic region is mainly exhibited in the centre of the vesicle. At the upper rim of the vesicle, the bilayer was not cleaved and the polar interface is exhibited. Clearly circular domains of one lipid component are formed in both monolayers. From the direction of the platinum shadow it follows that in the inner monolayer the domain are bent towards the interior of the vesicle. In the outer monolayer the domains are bent towards the outside. This is directly verified by a stereo-microscopic observation.

A different type of domain structure is shown in Fig. 8 for a membrane composed of 65% dioleyl phosphatidic acid (DOA), 15% dioleyl lecithin (DOL) and 20% cholesterol (at pH 9). Circular domains are formed with a diameter of the order of 500 Å. Such circular domains are expected to be formed if the lipid phase in the domain is of the smectic A or smectic B_A type and if the domain is formed in one monolayer only.

IV. Discussion of Domain Structure and Local Curvature

A) Thermodynamics of lateral phase separation

The combination of spectroscopy and electron microscopy has shown that lateral lipid separation is a common phenomena in two dimensional smectic phases of binary mixtures. In summary we come to the following conclusion:

1) Two dimensional smectic phases of different symmetry have an intrinsic tendency to separate laterally. The separation of smectic mesomorphic states of different symmetry is a well known phenomena in liquid crystal physics discovered by H. Sackmann and Demus [9]. In fact this finding has become a main tool for the classification of different types of smectic liquid crystals. It has been pointed out by de Gennes [19] that partial immiscibility of liquid crystalline phases of different symmetry is a natural consequence of a general rule of Landau and Lifshitz. This rule states that two phases of different symmetry must be separated by at least one phase transition line. A mixture of a tilted (compound in smectic C) and a nontilted (compound in smectic A) phase thus exhibits a "phase separation type" of first order transition.

2) Two phases of equal symmetry (*e. g.* smectic A) may, however, also be partially immiscible if they are composed of two compounds with different molecular shape or internal molecular symmetry [10]. This general principle most probably leads to the lateral segregation of the quasi-neutral DPL and the twofold charged DPA when both are in the smectic A phase [17]. The two molecules differ in the structure of the polar head group.

3) The above mentioned type of *chemical* phase separation in binary mixtures leads to two phases (denoted as $\oplus$ and $\ominus$) which differ in chemical composition. Each phase is characterized by a composition variable, η_+ and η_-, which may be considered as an order parameter. η is defined as the difference in molar fractions, x, of the two components a and b $[\eta_\pm = \pm (x_a - x_b)]$.

A second type of *physical* phase separation is also possible in one-component systems. The two different phases are distinguished physically. An important example is a membrane with biaxial symmetry where the molecules are tilted. The two phases are distinguished by the direction of the tilt *.

The order parameter is defined by the tilt angle Θ. The situation is illustrated schematically in Fig. 9 a. The free energy $f(\eta)$ of the generallized two phase system is plotted in Fig. 9 b as a function of

* In principle the free energy function, f, is rotational symmetric with respect to its symmetry axis. Therefore an infinite number of phases are possible. It is easily verified that for topological reasons only one pair of phases as shown in Fig. 9 a has to be considered.

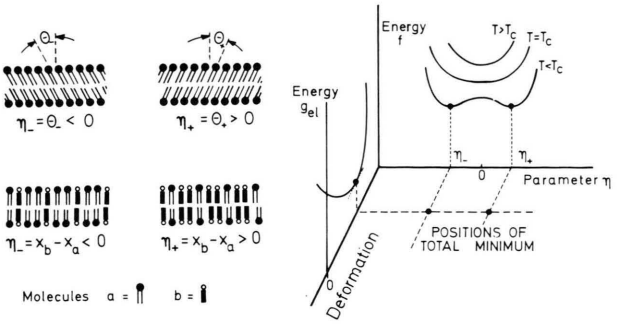

Fig. 9. Illustration of chemical and physical phase separation. a. Schematic representation of chemical and physical type of phase separation. In the case of the chemical type, a laterally ordered phase is shown. In fluid membranes this order will be broken down while the order parameter η is still defined. b. Free energy plotted as a function of order parameter η for a temperature below ($T<T_c$), at ($T=T_c$) and above ($T>T_c$) the critical temperature T_c. The order parameters for the minima of f (at $T<T_c$) are η_+ and η_-, respectively. In order to account for elastic contributions, g_{el}, a third dimension has been included which accounts for the elastic variable: "Deformation".

order parameter η. Phase separation is expected at $T<T_c$ where the free energy curves exhibit two minima. That region of the order parameters, η, where $\partial^2 f/\partial\eta^2<0$ is called the spinodal. This generalized scheme is the basis for our model of domain structure discussed below (*cf* chapter IV C and IV D). It should be emphasized that the above consideration is valid for an undistorted infinite system but does not include the possibility of domain formation. For the explanation of domain structure we have to take into account a further physical principle. This is provided by the membrane elasticity discussed in the following sub-section.

B) Orientational elasticity and local curvature

According to the elastic theory of lipid bilayers by Helfrich [29], the curvature of membranes is determined by the elastic energy connected with the spontaneous orientation of the lipid molecules. The curvature may be expressed in terms of the lateral variation of the vector L normal to the membrane surface (*cf* Fig. 10). If the components of L in the plane of the membrane are L_x and L_y, the curvature elastic energy per unit area for a uniaxial membrane is [29]

$$g_{el} = K_1\left(\frac{\partial L_x}{\partial x}+\frac{\partial L_y}{\partial y}\right) + \frac{1}{2}K_{11}\left(\frac{\partial L_x}{\partial x}+\frac{\partial L_y}{\partial y}\right)^2+\ldots\ldots \quad (1)$$

K_{11} is the splay elastic constant well known in liquid crystal physics [10]. The second quadratic term in Eqn (1) describes the deformation of the lipid bilayer under the influence of external forces. The first (linear) term takes account of the equilibrium form of a membrane (*e. g.* a vesicle):

Minimizing the elastic energy density leads to

$$\left(\frac{\partial L_x}{\partial x}+\frac{\partial L_y}{\partial y}\right)=c_0=-\frac{K_1}{K_{11}}. \quad (2)$$

c_0 describes the spontaneous curvature and was introduced by Helfrich [29]. In a fluid membrane g_{el} is the predominant contribution to the total elastic energy **.

The total free energy of a membrane is the sum of the thermodynamic potential f of Fig. 9 b and of the elastic energy g_{el} (per unit area):

$$F_{tot}=f+g_{el}.$$

Fig. 9 b has therefore been expanded in a third dimension by introducing as a further variable the elastic deformation. Minimizing this total free energy should then lead to the distorted configuration of a mixed membrane, that is the domain structure.

For a bilayer with *transverse asymmetry* c_0 is non-zero. Transverse asymmetry may be realized either by a different lipid composition of the two opposing monolayers or by a different composition of the aqueous phases on either side of the membrane. For bilayers with *transverse symmetry* the lateral average of c_0 has to be zero. Even in this case the membrane may exhibit locally transverse asymmetry. This would then also lead to a modulation in local curvature.

In the following several possible types of domain structure accompanied by a change in local curvature are summarized:

a) One component systems: According to Fig. 3 and Fig. 7, one-component lipid bilayers may exhibit a domain structure with periodic variation in local curvature. This was concluded from the fact that freeze etching electron microscopy is only sensitive to variation in local curvature. A closer inspection of the electron micrographs strongly suggests that the cross section of the elongated ripples is nearly triangular (*cf* Fig. 10). A model of this type

** In biaxial membranes (*e. g.* sm C) the elastic energy is more complex. For the present discussion Eqn (2) describes the basic effect.

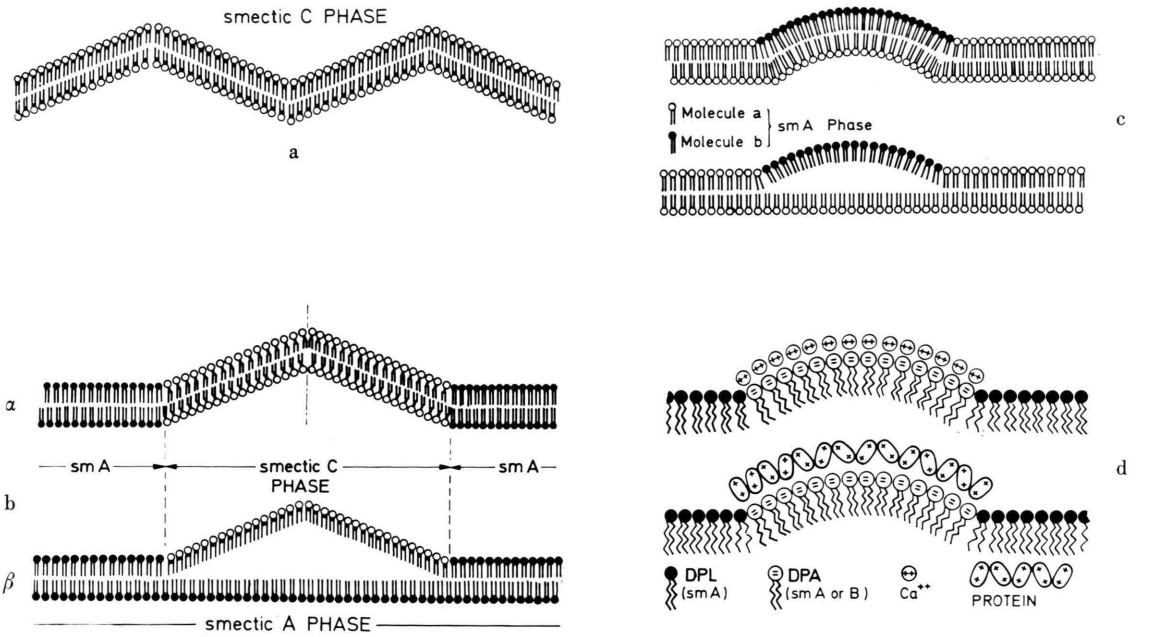

Fig. 10. Different types of local curvature in membranes with domain structure. a. One component system or random mixture. The triangular cross-section is suggested by the defect structure (*cf* Fig. 3 and Section IV E). b. Mixture of tilted and non-tilted phases: Two possibilities are conceivable: α) transversal symmetric (coupled monolayers) and β) transversal asymmetric (non-coupled) distribution of phases. Elongated domains are expected. c. Mixture of non-tilted phases of different composition. Again two cases are possible: transversal symmetric and asymmetric phase distribution. The second case is realized in Fig. 8. Circular domains are expected. d. Two possibilities of charge induced domain structure (*cf* ref. 24 and Fig. 3 of ref. 27).

of domain structure is given below (section IV D and E).

b) Mixed systems: Some types of domain structure that are expected in this case are also summarized in Fig. 10.

Fig. 10 a: Random mixture forming a smectic C phase: An identical structure as in the one component case is obtained.

Fig. 10 b: Phase separation between tilted (sm C or sm B_C) and non-tilted (sm A or sm B_A) smectic states: Two possibilities have to be considered:

Transversal symmetric distribution of phases allows domain formation where both monolayers are involved. Transversal asymmetric phase distribution can lead to a domain in one monolayer only. The latter domain type may form if the lipid hydrocarbon chains or some small impurity molecules may fill out the pocket created between the two monolayers.

In both cases elongated domains are expected to be formed. The reason for this is that the domain growth in biaxial membranes is highly anisotropic. According to Fig. 7 b, this type of domain structure is formed in mixed bilayers of lecithins and cholesterol. Wrinkle-like domains are clearly visible if DML/cholesterol lamellae are cooled from a temperature where DML is in the smectic B_C state. The same type of domains have been observed in our laboratory in pure lecithin membranes in the region of the sm A → sm B_{CA} transition (*e. g.* DPL vesicles at 40 °C) *.

Fig. 10 c: Phase separation in non-tilted smectic mixtures: As mentioned above, the domains are only visible in the electron microscope if they involve a change in local curvature. This implies that the transversal lipid distribution within the domains must be asymmetric. Circular clusters are expected to be formed since in uniaxial membranes the domain growth is isotropic. Two cases have to be distinguished again:

1) Domain formation in one monolayer only that is accompanied by the creation of a pocket, or
2) matching of the local curvature in both monolayers of the domain region.

* In this critical region the transverse transport properties of membranes may be drastically increased [31].

An example for this type of domain structure was shown in Fig. 8. A further important example for the circular type of domain is observed in the case of charge induced lateral phase separation illustrated in Fig. 10 d. This mechanism of domain formation was reported in detail previously [24].

C) Dynamics of domain structure

A surprising result of the spectroscopic study is the finding that a mosaic-like lipid distribution may be found if both lipid components are in a fluid state. Examples are the DPA/DPL mixture above 47 °C (at pH 9) and the DPL/DOL mixture at $T > 42$ °C [27]. It should be emphasized, however, that in ESR-spectroscopy time averages of lipid distribution are measured. The lifetime of a domain of labelled lipid should be larger than the reciprocal of the exchange frequency which is of the order of 10^{-7} sec.

Now, the kinetics of domain formation and decay may be estimated by application of the theories on spinodal decomposition by Cahn [33] and by Langer [34]: Consider a flat membrane composed of a lipid mixture. Assume that a periodic (plane wave) variation in concentration, characterized by a wavelength Λ, is built up after adjusting the external condition (temperature, pH) in such a way that the mixed system starts to decompose into two phases. According to Cahn's theory, the lipid domains grow exponentially with a time constant, τ, given by

$$\frac{1}{\tau} \approx \frac{1}{2} D \left(\frac{2\pi}{\Lambda} \right)^2 .$$

D is the coefficient of lipid lateral diffusion. For fluid (sm A) bilayer, D is of the order of $D \approx 10^{-7}$ cm^2/sec [17]. Domains of wavelength $\Lambda \sim 100$ Å could thus form within $\tau \sim 10^{-6}$ sec. This result shows that domain formation may be a very fast process. It is, however, slow compared to the time scale important in ESR-spectroscopy. If one of the phases is of the rigid smectic B type, the rates of domain formation and decay may be several orders of magnitude slower.

D) Models of domain structure

The above consideration shows that the domain pattern is at least a metastable state of lipid alloys. In the following we present simple models of domain structure for both pure and mixed lipid lamellae.

a) Domain structure of lipid mixtures: Upon cooling a two-dimensional lipid alloy below the critical temperature, T_c, phase separation is usually expected to start as a spinodal decomposition. The initial state may be described in terms of a plane wave fluctuation in concentration: $\eta = \eta_0 \cdot \cos k_0 x$ with $k_0 = 2\pi/\Lambda$. The x-axis lies within the average membrane surface. The subsequent coarsening process leads to an increase in wavelength and the formation of sharp interfaces between the different phases. The lateral organization of the phases is determined by 3 energetic contributions:

1) The gain in free energy upon phase separation. In the approximation of the mean field theory this excess energy density is given by [33, 36]

$$E = \nu_{ab} \frac{2 k T_c}{Z} . \qquad (3\,a)$$

ν_{ab} is the average number of nearest-neighbor pairs formed between the two different species (a and b). $Z = 6$ for a hexagonal lattice.

Near the critical temperature, T_c [36],

$$\nu_{ab} \approx \frac{N_L \cdot Z}{4} (2 - 3\,T/T_c) \qquad (3\,b)$$

where N_L is the number of lipids per unit area.

2) The expense of chemical free energy, necessary to form an interface of non-equilibrium composition. According to Cahn's theory [33] this "chemical" interfacial energy per unit area is

$$\sigma_{chem} = \varkappa \cdot (d\eta/dx)^2 . \qquad (4\,a)$$

Now, Cahn has shown that this expression determines the thickness of the interface. In the vicinity of T_c the width of the interface is given by

$$\Delta\varrho = 2\lambda \sqrt{T_c/(T_c - T)} \qquad (4\,b)$$

where λ is the average nearest neighbor distance.

3) The elastic interfacial energy due to the difference in spontaneous curvature of the two different phases. Consider the plane-wave domain structure with domains of width ϱ. The elastic energy may be expressed as a power series of the gradient in curvature as follows:

$$g_{el} = \frac{1}{2} \frac{r_I^4 K_{11}}{(dr_I/dx)^2} \varrho^2 = \gamma_{el} \cdot \varrho^2 . \qquad (5)$$

r_I is the spontaneous curvature of the domain I (*cf* Fig. 11) as determined by the linear term in Eqn (2). In the present model r_I and r_{II} are fixed in the domain, while $dr_I/dx \neq 0$ in the interfacial

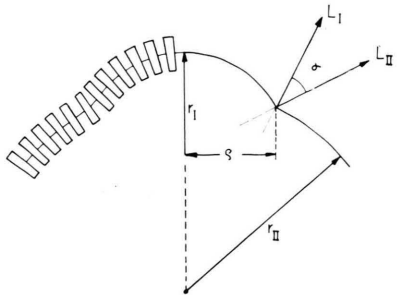

Fig. 11. Formation of alternating regions with a large $(1/r_I)$ and a small spontaneous curvature $(1/r_{II})$. The directors normal to the membrane surfaces, L_I and L_{II}, form an angle α. This is the source of splay deformation at the interface of the two phases.

region. It is characteristic for the Cahn model that $\Delta\varrho$ is considerably larger than the average lipid distance. The simplest approximation is a linear variation in r within the interfacial region. One then obtains $dr_I/dx \approx (r_{II} - r_I)/\Delta\varrho$.

For a 1 : 1 mixture and for a plane wave domain pattern of equal domain width, the total free energy per unit area is:

$$F_{tot} = \frac{2E \cdot \varrho}{\varrho + \Delta\varrho} + \frac{\gamma_{el}\,\varrho^3}{\varrho + \Delta\varrho} + \frac{\sigma_{chem}}{\varrho + \Delta\varrho}. \quad (6\,a)$$

Minimizing F_{tot} with respect to the domain width ϱ yields

$$\varrho_0 = \Delta\varrho\left(1 + \sqrt{1 + \frac{E\,\Delta\varrho + \sigma_{chem}}{\gamma_{el} \cdot \Delta\varrho^2}}\right). \quad (6\,b)$$

An estimation shows that σ_{chem} is about 100 times smaller than $E \cdot \Delta\varrho$. The 2nd term under the square root is large compared to 1 and gives the main contribution to ϱ_0. In the vicinity of the critical temperature $(T - T_c \ll T)$ it follows

$$\varrho_0 \approx \frac{\lambda}{\Delta c}\sqrt{\frac{4\,k\,T_c\,N_L}{K_{11}} \cdot \frac{T}{T_c - T}}, \quad (6\,c)$$

by inserting Eqns (3 a), (3 b) and (4 b).

Here $\Delta c = r_I^{-1} - r_{II}^{-1}$. For $\Delta c \to 0$ $(\varrho \to \infty)$, a lateral separation of the two phases on a macroscopic scale is expected. For $\Delta c \neq 0$, ϱ decreases rapidly with $T - T_c$.

Consider a mixture of lecithin (DPL) and phosphatidic acid (DPA). Our experimental studies of sonicated vesicles suggest a value of $\Delta c \approx 5 \times 10^{+2}\,cm^{-1}$, since $r_{DPL} \approx 400$ Å; $r_{DPA} \approx 200$ Å. The area per lipid molecule of 60 Å^2 yields $N_L = 1.6 \times 10^{14}\,cm^{-2}$ and $\lambda \sim 7.7$ Å. For $K_{11} \approx 2 \times 10^{-12}$ erg [38], $T_c = 320$ K one obtains for a temperature of 5 °C below T_c a value of $\varrho \approx 300$ Å. This value is in good agreement with the experimental domain width of about 400 Å found in Fig. 7 b and in Fig. 8.

b) Domain structure of pure lipid: Provided the two monolayers of a lipid bilayer are decoupled, each monolayer tends to exhibit a spontaneous curvature (*cf* Fig. 12). The width, $\varrho + \Delta\varrho$, of the

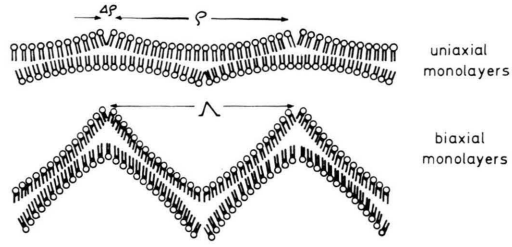

Fig. 12. Schematic representation of spontaneously curved monolayers of lipid bilayers leading to the rippled structure.

domains is assumed to be determined by the following factors:

1. The gain in free energy by the spontaneous curvature.
2. The expense in compression energy due to the increase in membrane thickness caused by the spontaneous curvature (*cf* Fig. 12).
3. The expense in Cahn type of interfacial energy.

The last contribution is small compared to the compression energy and is therefore neglected. Assuming that the spontaneous curvature, $1/r$, is constant, the total energy density is:

$$F_{tot} = \frac{K_1}{r}\left(\frac{\varrho}{\varrho + \Delta\varrho}\right) + \frac{1}{2}\frac{K_{11}}{r^2}\left(\frac{\varrho}{\varrho + \Delta\varrho}\right) + \frac{1}{5}\left(\frac{\varrho}{8}\right)^5 (\varrho + \Delta\varrho)^{-1}\frac{K_{comp}}{r^2 \cdot d^2} + \frac{\sigma_{chem}}{\varrho + \Delta\varrho}. \quad (7)$$

K_{comp} is the transversal compressibility of the bilayer and d is its average thickness. Minimizing F_{tot} both with respect to ϱ and $(1/r)$ yields two equations for the two unknowns ϱ and $1/r$. Elimination of $1/r$ yields

$$\frac{1}{2}K_{11}\,\Delta\varrho + \frac{1}{5 \cdot 8^5}\frac{K_{comp}}{d^2}(3\,\varrho^4\,\Delta\varrho + 4\,\varrho^5) = 0. \quad (8)$$

F_{tot} becomes negative if the domain width, ϱ_0, and the spontaneous radius r_0 obtained by the minimization procedure are inserted into Eqn (7). From the bulk compressibility of phospholipids one estimates

$K_{comp} \approx 200$ dyn/cm. For $d \approx 5 \times 10^{-7}$ cm one obtains $\varrho_0 \sim 60$ Å in resonable agreement with the experimental finding of $\varrho_0 + \Delta\varrho = 200$ Å (*cf* Fig. 3). Larger values of ϱ_0 are expected if σ_{chem} is taken into consideration. The above calculation is valid for sm A membranes. The out-of-plane distortion is

$$h_0 \cong \sqrt{\frac{20}{3}} \sqrt{\frac{K_{11}}{K_{comp}}} \frac{d}{r_0}.$$

For sm A one obtains $h_0 \approx 10$ Å and this is therefore not observable. However, for sm C systems the amplitude of the ripple structure is magnified according to

$$h \approx h_0 + \frac{1}{2} \varrho_0 \tan \Theta .$$

For a typical tilt angle $\Theta = 30^\circ$ one estimates $h = 80$ Å which is well consistent with the experimental finding **.

E) Defects of ondulated pattern — a symmetry rule

The periodic ripple pattern of a curved vesicle is not perfect. It will exhibit defects (*cf* Fig. 3). These defects are of special interest, since they may give information on the symmetry properties of the periodic distortion. From this, information on the average lipid orientation with respect to the membrane normal may be obtained. A typical defect of the ondulated structure is drawn schematically in Fig. 13. Now, introduce a vector $\boldsymbol{l}$ which lies in the

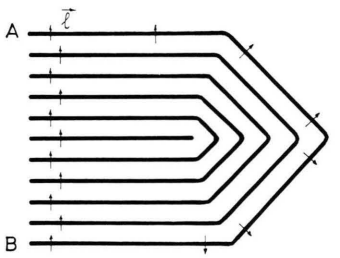

Fig. 13. Schematic representation of defects in the ondulated structure as seen in Fig. 3 and Fig. 7. One line represents the centre of the elongated domains.

average plane, E, parallel to the membrane surface that cuts the membrane into two identical parts. $\boldsymbol{l}$ is assumed to be oriented perpendicular to the ripples (*cf* Fig. 13). The length of $\boldsymbol{l}$ may be defined as

$$|\boldsymbol{l}| = \int_{\text{Periode}} \cdot \cos \Phi \, dx \qquad (15)$$

where Φ is the angle between the molecular orientation and E. $\boldsymbol{l}$ thus gives a measure for the net orientation per domain. If the vector $\boldsymbol{l}$ is moved around the defect from B to A (*cf* Fig. 13) along any ripple it is reversed ($\boldsymbol{l} \rightarrow -\boldsymbol{l}$). This leads to the conclusions: 1) The physical property described by the vector $\boldsymbol{l}$ must be polar, or 2) the vector $\boldsymbol{l}$ is zero. Now, a lateral asymmetric distortion for which $\boldsymbol{l} \rightarrow -\boldsymbol{l}$ (upon surrounding a defect), could only be possible in a multiple plane. The periodic distortion of a membrane must be laterally symmetric *.

As an example we may apply the above symmetry rule to the model of the ripple structure by Tardieu *et al.* [12]. These authors assume: 1) The periodic distortion is sinusoidal and 2) the orientation of the tilted lipids is fixed with respect to the normal of the membrane. Applying Eqn (15) to this model shows that $\boldsymbol{l}$ is not zero. Since $\boldsymbol{l} \rightarrow -\boldsymbol{l}$ is forbidden after the above symmetry rule the Tardieu model is not consistent with the observed defect structure.

The symmetry rule has been derived by considering the molecular orientation. It also applies to any other physical property projected onto the membrane plane E. Information on the membrane transverse symmetry cannot be obtained from the defect structure of the electron micrograph.

The polar head group region is also expected to obey the above symmetry rule. In addition, it may lead to a gain in free energy due to formation of an electric double layer. On the other hand, a high electrostatic energy density would be involved if sharp edges at the rim of the ripples would be formed. The polar head group region thus prevents sharp edges. This argument is valid both for charged head groups (*e. g.* phosphatidic acid) and dipolar groups (*e. g.* lecithins).

Appendix A

Fig. 14 shows an electron micrograph of a DML bilayer vesicle cooled very rapidly ($\sim 10^{+6}$ °C/sec) from the biaxial smectic B_c state. In contrast to the finding of the left side in Fig. 7 a, a defect structure is observed. It exhibits a spiral pattern and is thus clearly distinguished from the regular pattern of the ripple structure (Fig. 7 a, $T_1 < T < T_2$). This spiral pattern may be explained as follows: Consider a

** At this point we express our thanks to Prof. W. Helfrich for helpful remarks concerning the calculation of the domain width.

* Lateral asymmetric distortion would be possible for disclination lines or inversion walls.

biaxial bilayer vesicle with negligible spontaneous curvature. For topological reasons it is not possible to form a closed vesicle without defects: A first possibility is a homogenous lipid orientation all over the vesicle. This would lead to singularities in orientation at the two poles with a prohibitively high energy content. Another possibility would be to change the orientation upon approaching the poles

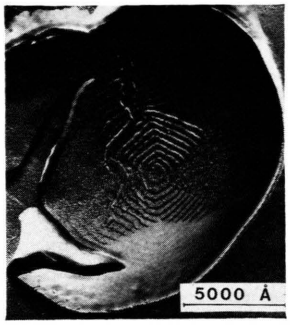

Fig. 14. Electron micrograph of a DML bilayer vesicle cooled very rapidly from the biaxial smectic B_Q state by shooting the vesicle preparation into the coolant. A screw dislocation is clearly seen which is reminiscent of the spiral growth pattern of crystals [40].

in such a way that there the orientation is parallel to the pole axis. Provided the membrane thickness is kept constant, the change in orinetation produces a curvature. This effect is very strong near the poles where a peak is expected to form. Inspection of the micrographs (*cf* Fig. 14) shows that such peaks are indeed formed in the centre of the spirals **.

The projection, $\boldsymbol{P}$, of the director of the lipid orientation on the membrane plane may be split up into vectors parallel ($\boldsymbol{P}_{\parallel}$) and perpendicular ($\boldsymbol{P}_{\perp}$) to the meridians of the vesicle. Far away from the poles a homogeneous orientation is possible. Upon following the projection vector, $\boldsymbol{P}$, one moves along a spiral towards the pole. Now, if the vesicle is subject to a high strain upon cooling, the bilayer is expected to break along the screw-like lipid orientation pattern. According to the above consideration a spiral pattern is only expected for biaxial membranes. A further characteristic property for the spiral pattern is its hexagonal symmetry. This additional feature is a consequence of the hexagonal crystal structure of the lipid bilayer.

** Such an escape of a disclination into the third dimension is also observed in nematic liquid crystals (see *e. g.* ref. 10 p. 133).

Appendix B: Surface Induced Domains in Ordered Fluids

The domain structure in membranes may be considered as a special case of the surface domain pattern which is often observed in thermotropic liquid crystals. In the present paper the domain structure was closely related 1) to the polarity of the lipid lamellae and 2) to the occurance of the generallized chemical and physical types of phase separation (*cf* Fig. 9). In ordinary 3-dimensional liquid crystals the physical type of phase separation could of course also occur.

At the phase transition smectic-A → smectic C and nematic → smectic C, completely different behavior is observed in the bulk and at the interface (*e. g.* air/liquid crystal). The bulk is usually charac-

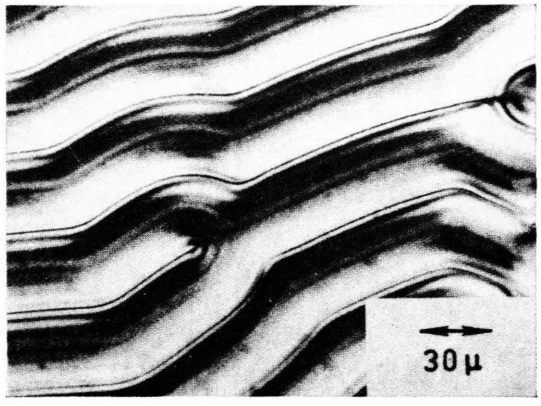

Fig. 15. Surface induced domain pattern at the air/liquid crystal interface of 4,4′-di-heptyloxyazoxybenzene in the temperature region of the nematic-smectic C transition. The domain structure is also stable with a different wavelength in the smectic C phase (according to ref. 41).

terized by the absence of polarity, and phase separation does not lead to a stable domain structure. Indeed, a domain structure in the bulk phase has not been observed yet. However, at the interface, air/liquid crystal, a domain pattern is often present. An example is shown in Fig. 15 for the nematic → smectic C transition [41]. A domain pattern induced by surface polarity has also been observed in thin layers of thermotropic smectic C liquid crystals [42].

The electron microscopy experiments were performed in the "Sektion für Elektronenmikroskopie" at the University of Ulm. We are most grateful to Prof. R. Martin for his generous help. To Dr. H. J.

Galla and to W. Hartmann we thank for helpful discussions and for allowing us to use experimental material of earlier work. One of us (C. Gebhardt) would like to express his thanks to the Lucas Meyer Company, Hamburg, for a fellowship. Finally we thank the Deutsche Forschungsgemeinschaft for the financial support (under contract No. Sa 246 and Gr 551).

[1] L. L. M. Van Deenen and J. de Gier, The Red Blood Cell (D. M. N. Surgenor, ed.), Academic Press, New York 1974.
[2] A. Stier and E. Sackmann, Biochim. Biophys. Acta **311,** 400 [1973].
[3] R. Peters, J. Peters, K. H. Tews, and W. Bähr, Biochim. Biophys. Acta **367,** 282 [1974].
[4] G. M. Edelmann, Science **192,** 218 [1976].
[5] A. Elgsaeter, D. M. Shotton, and D. Branton, Biochim. Biophys. Acta **426,** 101 [1976].
[6] U. C. Philips, R. M. Williams, and D. Chapman, Chem. Phys. Lipids **3,** 234 [1969].
[7] B. D. Ladbrooke, R. M. Williams, and D. Chapman, Chem. Phys. Lipids **1,** 445 [1967].
[8] W. Helfrich, VI. International Liquid Crystal Conference 1976, Kent (Ohio) USA.
[9] H. Sackmann and D. Demus, Mol. Cryst. **2,** 81 [1966].
[10] P. G. de Gennes, The Physics of Liquid Crystals, 2nd ed., Clarendon Press, Oxford 1974.
[11] E. Sackmann and H. Träuble, J. Amer. Chem. Soc. **94,** 4482 [1972]; J. Amer. Chem. Soc. **94,** 4499 [1972].
[12] A. Tardieu, V. Luzzati, and F. C. Reman, J. Molec. Biol. **75,** 711 [1972].
[13] L. Powers and N. A. Clark, Proc. Natl. Acad. Sci. **72,** 840 [1975].
[14] M. J. Janiak, G. G. Shipley, and D. M. Small, VI. International Liquid Crystal Conference, 1976, Kent, Ohio, USA.
[15] A. J. Verkleij, P. H. J. Ververgaert, and L. L. M. van Deenen, and P. F. Elbers, Biochim. Biophys. Acta **228,** 326 [1972].
[16] H. J. Eibl and H. Träuble, Proc. Nat. Acad. Sci. U.S. **71,** 214 [1972].
[17] H. J. Galla and E. Sackmann, J. Amer. Chem. Soc. **97,** 4114 [1975].
[18] K. Jacobsen and D. Papahadjopoulos, Biochemistry **14,** 152 [1975].
[19] J. Luisetti, unpublished results.
[20] J. P. Reeves and R. M. Dowben, J. Cell Physiol. **73,** 49 [1969].
[21] E. Sackmann, Z. Phys. Chem. NF **101,** 391 [1976].
[22] E. J. Shimshick and H. M. McConnell, Biochemistry **12,** 2351 [1973].
[23] A. G. Lee, N. J. M. Birdsall, J. C. Metcalf, P. A. Toon, and G. B. Warron, Biochemistry **13,** 3699 [1974].
[24] H. J. Galla and E. Sackmann, Biochim. Biophys. Acta **401,** 509 [1975].
[25] W. Kleemann and H. M. McConnell, Biochim. Biophys. Acta **345,** 220 [1974].
[26] E. Sackmann, O. Albrecht, H. J. Galla, and W. Hartmann, Structural and Kinetic Approach to Plasma Membrane Function, 1976, Grignon, France, in press.
[27] W. Hartmann, H. J. Galla, and E. Sackmann, to be published.
[28] W. Helfrich, Z. Naturforsch. **28 c,** 693 [1973].
[29] H. Gruler, Z. Naturforsch. **30 c,** 608 [1975].
[30] H. M. McConnell, C. W. Grant, S. Hong-Wei Wu, and H. McConnell, Biochim. Biophys. Acta **363,** 151 [1974].
[31] D. Marsh, A. Watts, and P. F. Knowles, Evidence for Phase Boundary: Permeability of TEMPO-Choline into DML Vesicles at the Phase Transition, Biochim. **15,** 3570 [1976].
[32] W. Pjura and H. Gruler, to be published.
[33] J. W. Chan, Trans. Metallurgical Soc. AIME **242,** 166 [1968].
[34] J. S. Langer, Annals of Physics **65,** 53 [1971].
[35] O. H. Griffith, P. Jost, R. A. Capold, and G. Vanderkooi, Ann. New York Acad. Sci. **222,** 561 [1973].
[36] R. Becker, Theorie der Wärme, Springer Verlag, Berlin 1966.
[37] S. Marcelja, Biochim. Biophys. Acta **455,** 1 [1976].
[38] W. Helfrich and S. Marcelja, will be published.
[39] H. Gruler and E. Sackmann, to be published in Croatica Chemica Acta **49,** 379 [1977].
[40] C. Kittel, Introduction to Solid State Physics, 4th Ed., p. 691, J. Wiley & Sons, New York 1971.
[41] T. J. Scheffer, H. Gruler, and G. Meier, Solid. State Comm. **11,** 253 [1972].
[42] R. B. Meyer and P. S. Pershan, Solid State Comm. **13,** 989 [1976].